physica status solidi a
www.pss-a.com
applications and materials science

Radiation-induced interstitial carbon atom in silicon: Effect of charge state on annealing characteristics

Stanislau B. Lastovskii[**,1], **Vasilii E. Gusakov**[1], **Vladimir P. Markevich**[*,2], **Anthony R. Peaker**[2], **Hanna S. Yakushevich**[1], **Fedor P. Korshunov**[1], and **Leonid I. Murin**[1]

[1] Scientific-Practical Materials Research Center of NAS of Belarus, 220072 Minsk, Belarus
[2] Photon Science Institute and School of Electrical and Electronic Engineering, University of Manchester, Manchester M13 9PL, UK

* Corresponding author: e-mail v.markevich@manchester.ac.uk, Phone: +44 161 306 4746
** e-mail lastov@ifttp.bas-net.by, Phone +375 17 284 1289, Fax: +375 17 284 1528

We present experimental and theoretical results showing that the migration of interstitial carbon atom (C_i) in silicon depends on its charge state. The experimental results were obtained from the analysis of changes in concentrations of the C_i defect, which were determined from deep level transient spectra, in n^+-p diodes subjected to irradiation with 4–6 MeV electrons or α-particles at $T \leq 273$ K and subsequent heat-treatments in the temperature range 280–330 K with applied reverse bias voltage and without it. It has been found that in the positive charge state the C_i migration energy is 0.88 ± 0.02 eV, while in the neutral charge state it is reduced to 0.73–0.74 eV.

First-principles density-functional calculations of the structure of C_i in different charge states ($z = 0, +1, -1$) and diffusion coefficient parameters (activation barrier ΔE_a and pre-exponential factor D_0) have been performed. It has been found that a split-$\langle 100 \rangle$ configuration with C_{2v} symmetry is the most stable one for C_i in all the charge states. The following ΔE_a and D_0 values have been derived from the calculations: $\Delta E_a = 0.74$ eV and $D_0 = 0.06$ cm^2 s^{-1} for C_i^0, and $\Delta E_a = 0.89$ eV for C_i^+.

1 Introduction Carbon is an important technological impurity in silicon [1, 2]. In commercial Si crystals, carbon atoms are present in concentrations typically in the 10^{15} to 10^{16} cm^{-3} range and in as-grown material are located mainly at substitutional (C_s) sites. Substitutional carbon atoms are well known to be effective traps for silicon self-interstitials. Interstitial carbon atoms (C_i) formed via the Watkins replacement mechanism are among the main radiation-induced defects in irradiated Si crystal [1, 3–6]. The C_i defect was observed and identified with the use of various experimental techniques: i) infrared absorption (IR) spectroscopy (the most intense local vibrational mode (LVM) lines at 922 and 932 cm^{-1} [3, 5]), ii) electron spin resonance (Si-G12 and Si-L6 signals [7, 8]), iii) Hall effect and deep level transient spectroscopy (energy levels at about $E_C - 0.12$ eV and $E_V + 0.28$ eV) [4, 8–14]), and iv) photoluminescence (line with $h\nu = 856$ meV [15]).

However, in spite of numerous studies of the C_i defect, some questions related to the mechanism of its disappearance upon annealing are still under debate. The defect is mobile at room temperatures and can interact with many impurities and defects forming various complexes (C_iC_s, C_iO_i, C_iP_s, etc.) [1]. On the other hand, there is no consensus regarding the effect of the C_i charge state on the defect annealing characteristics. In the present work, we will review the results previously published in this field [4, 7–13, 16–18] considering the charge state effects. It should be noted that it has been stated in some papers that the C_i diffusivity is almost the same for the defect in different charge states [8, 16] and this opinion has been widely accepted. In the present work, we will present experimental and theoretical evidences showing that the migration of C_i depends very significantly on its charge state.

2 Experimental and modeling details

Experimental results in the present work were obtained from DLTS and high-resolution Laplace DLTS (L-DLTS) [19] measurements on n^+-p-p^+ diodes. Two sets of n^+-p-p^+ diodes were prepared. One set of the diodes was produced on boron-doped epi-Si ($\rho \approx 20\,\Omega \cdot cm$), which was grown on highly boron-doped ($\rho \approx 0.005\,\Omega \cdot cm$) Czochralski-grown (Cz) Si wafers. The diodes were formed by implantation of phosphorus ions with a subsequent annealing at $1150\,°C$ in a nitrogen-oxygen gas ambient. N^+-p-p^+ diodes from another set were prepared by phosphorus diffusion at about $1000\,°C$ from PCl$_3$ gas ambient into a boron-doped ($\rho \approx 5\,\Omega \cdot cm$) Cz-Si wafer with an initial oxygen content of $7.5 \times 10^{17}\,cm^{-3}$. The back side of the wafer was boron implanted followed by laser annealing in order to create a p^+ layer for contacting. Oxygen concentrations in the epi-layers were estimated from the rate of transformation of the divacancy (V_2) to the divacancy-oxygen defect with the use of data presented in Ref. [20]. The oxygen concentration was $(3–4) \times 10^{17}\,cm^{-3}$ in the epi-Si diodes.

The samples were irradiated with 4 MeV electrons at $T \approx 280\,K$ with the use of a linear accelerator. The flux of electrons was $1 \times 10^{12}\,cm^{-2}\,s^{-1}$. Some samples were irradiated with α-particles from a Pu-239 surface source at 280–290 K. The α-particle energies were 5.144 and 5.157 MeV.

To determine the C_i annealing characteristics for the different charge states of the defect the irradiated n^+-p-structures were subjected to various isochronal and isothermal anneals in the temperature range 280–330 K under different bias conditions. Two main regimes were used: annealing with an application of reverse bias (7–30 V) when C_i was in the neutral charge state and annealing without bias when in the $5\,\Omega \cdot cm$ p-Si crystals the interstitial carbon was mainly positively charged.

The theoretical analysis of the structure of C_i in different charge states ($z = 0, +1, -1$), the corresponding normal modes of vibrations and diffusion coefficient parameters (activation barrier ΔE_a and pre-exponential factor D_0) has been performed. The first-principles density-functional calculations were carried out using the Quantum ESPRESSO package within the LSDA and B3LYP approximation to the exchange-correlation potential [21]. The crystal was modeled with either 64 or 216 Si atoms periodic supercells.

3 Results and discussion

3.1 Experimental results

Radiation-induced defects in the p-type Si crystals were characterized by means of DLTS and L-DLTS with a focus on the C_i donor level. The values of activation energy for hole emission and the pre-exponential factor have been determined for this level from an Arrhenius plot of T^2-corrected emission rates as $0.292 \pm 0.002\,eV$ and $1.6 \times 10^7\,s^{-1}\,K^{-2}$, respectively. The directly measured hole capture cross section for C_i in the neutral charge state was found to be $\sigma_p = 3.4 \times 10^{-15} \exp[-0.024\ (eV)/kT]\,cm^2$. The values of enthalpy and entropy of ionization for the C_i donor level have been calculated as $\Delta H(0/+) = 0.266\,eV$ and $\Delta S(0/+) = -0.19\,k\,eV \cdot K^{-1}$. With these ΔH and ΔS values the free energy of ionization, $\Delta G(0/+) = \Delta H(0/+) - T\Delta S(0/+)$, and the position of the defect energy level in the gap, $E(0/+) = E_V + \Delta G(0/+)$, were determined. The $E(0/+)$ level of the C_i defect has a weak temperature dependence and in the region of room temperatures it is located at about $E_V + 0.27\,eV$. The level position agrees well with the data obtained earlier by the means of the Hall effect measurements [22]. Using this position of the C_i donor level we have calculated the temperature dependencies of hole occupancy function of the level $N^+/N = 1/\{1 + \exp[(-0.27\ (eV)/kT] \times N_V/p\}$ in the p-type Si crystals. Figure 1 shows the C_i hole occupancy functions for p-type Si crystals with different doping levels ($[B_s] = 3 \times 10^{13} - 5 \times 10^{15}\,cm^{-3}$). When calculating these dependencies the values of effective density of states in the valence band were taken as $N_V = 8.1 \times 10^{14} \times T^{1.85}\,cm^{-3}$ according to the data by Green [23]. As can be seen, in samples with low resistivity (high $[B_s]$ values) the majority of C_i atoms are positively charged in the temperature range close to room temperature.

There is a commonly used approach in the studies of defect charge state effects on the defect annealing characteristics. This approach is based on application of the reverse bias to p-n-structures during thermal anneals. Examples of such an approach are studies of the elimination of the phosphorus-vacancy complex in silicon [24–27].

Figure 2 shows changes in remaining fraction of the C_i defect in the electron-irradiated Si n^+-p diodes ($[B_s] = 2.5 \times 10^{15}\,cm^{-3}$) upon their 15-min isochronal annealing under different bias conditions: $1 - U_b = 0\,V$, $2 - U_b = -20\,V$. An analysis of the DLTS spectra measured after different annealing steps has shown that in both cases there is almost one to one transformation of C_i into the C_iO_i defect. In agreement with previous studies (see Ref. [1] and references therein), these results indicate that the C_i defect is mobile at $T > 280\,K$ and in the material studied is captured by interstitial oxygen atoms when traveling along the Si lattice.
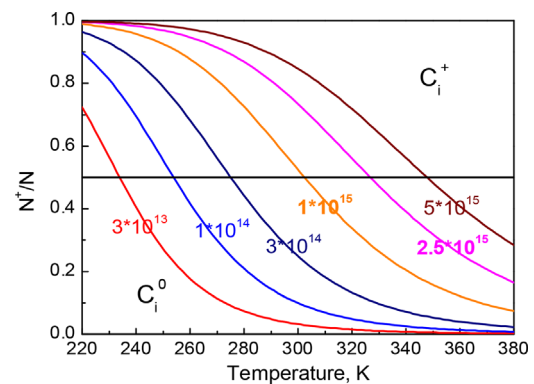

Figure 1 Occupancy function of interstitial carbon donor level for p-Si crystals with different doping level. Concentrations of holes are indicated on the curves. N means a total concentration of the defect: $N = N^+ + N^0$.
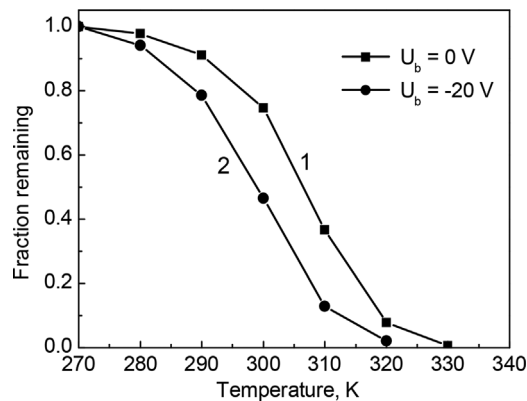
Figure 2 Changes in the remaining fraction of the C_i defects in the electron-irradiated ($E = 4$ MeV, $F = 3 \times 10^{15}$ cm^{-2}) Si n$^+$-p diodes ([B$_s$] $= 2.5 \times 10^{15}$ cm^{-3}) upon their 15-min isochronal annealing under different bias conditions: $1 - U_b = 0$ V, $2 - U_b = -20$ V.

However, the rate of the $C_i + O_i \Rightarrow C_iO_i$ transformation is noticeably higher in the sample annealed under -20 V bias. In this case, the C_i defect was in the neutral charge state while at $U_b = 0$ V the main part of the defect was positively charged at $T < 320$ K (see the curve for $p = 2.5 \times 10^{15}$ cm^{-3} in Fig. 1).

Figure 3 shows changes in the remaining fraction of the C_i defects in the alpha-irradiated Si n$^+$-p diodes with lower content of boron ([B$_s$] $= 5 \times 10^{13}$ cm^{-3}) upon their 15-min isochronal annealing under different bias conditions: $1 - U_b = 0$ V, $2 - U_b = -10$ V. For these samples, the rate of C_i annealing appears to be almost independent of the bias conditions. Evidently, at both annealing regimes the main charge state of C_i is the neutral one in the investigated range of temperatures in this material.

To determine more precisely the C_i annealing characteristics in the positive and neutral charge states, the electron irradiated n$^+$-p-structures ([B$_s$] $= 2.5 \times 10^{15}$ cm^{-3}) w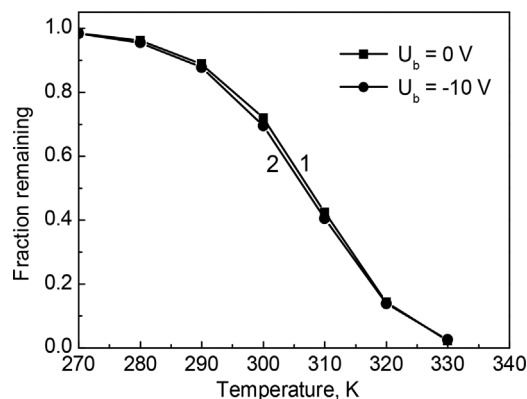ere subjected to isothermal anneals in the temperature range 280–330 K under different bias conditions. Two main regimes were used again: annealing with an application of a reverse bias (-20 V) when C_i was in the neutral charge state and without bias when in the studied p-Si crystals interstitial carbon was mainly positively charged. The studies performed have shown that there is a mono-exponential decay of the C_i concentration versus the annealing duration. The mono-exponential decay process allows an easy determination of the characteristic time $\tau = \nu^{-1} \times$ exp-($\Delta E/kT$) of the C_i disappearance. The values of τ were determined for temperatures in the range 280–335 K and are shown in Fig. 4 as Arrhenius plots together with the fitting lines for the samples annealed under different bias conditions. From an analysis of the data obtained it has been found that in the positive charge state the C_i migration energy is 0.885 ± 0.015 eV with $\nu = 1.6 \times 10^{11}$ s^{-1}, while in the neutral charge state it is lowered down to 0.74 ± 0.02 eV with $\nu = 1.4 \times 10^9$ s^{-1}. It should be pointed out that the C_i annealing rate under reverse bias was independent on the value of bias (7, 20, or 30 V).

The derived values are consistent with the majority of the results on the C_i elimination published previously (see Table 1). A more detailed discussion of some differences between our results on the annealing characteristics of C_i and the results on the subject, which were obtained in the previous studies, will be published elsewhere.

3.2 Modeling results For the simulation of the effect of defect charge states on diffusion coefficient parameters, we first of all performed a detailed analysis of an equilibrium position of interstitial carbon atom in the Si crystal lattice. The calculations were carried out in a cluster approximation with the use of a Si$_{59}$H$_{60}$C cluster (basis 6-31G with LSDA, B3LYP, HCTH approximations of the exchange-correlation energy), and with the use of Si$_{64}$ and Si$_{216}$ periodic supercells with LSDA and B3LYP
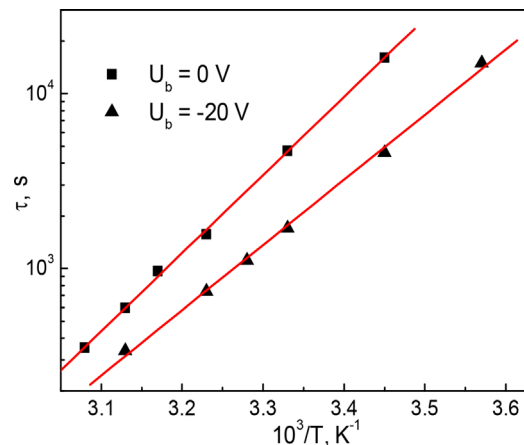

Figure 3 Changes in remaining fraction of the C_i defects in the alpha particle-irradiated Si n$^+$-p diodes ([B$_s$] $= 5 \times 10^{13}$ cm^{-3}) upon their 15-min isochronal annealing under different bias conditions: $1 - U_b = 0$ V, $2 - U_b = -10$ V.

Figure 4 Arrhenius plots of characteristic time of the C_i annihilation in electron-irradiated Si n$^+$-p diodes ([B$_s$] $= 2.5 \times 10^{15}$ cm^{-3}) which were annealed isothermally with reverse bias of -20 V or without bias.

Table 1 Previous studies: the C_i annealing characterization.

reference	method	material	temperature range, K	ΔE, eV	v, s^{-1}
[4]	DLTS	n-Si, $[P_s] = 2 \times 10^{12}$ cm^{-3}	313–333	0.72 ± 0.05	
[7]	EPR, reorientation	p-Si, $[B_s] = 10^{15}$ cm^{-3}	208–222	0.88	1.1×10^{16}
[8]	DLTS	n-Si, $[P_s] = 1 \times 10^{15}$ cm^{-3}	320–345	0.74	5×10^7
		p-Si, $[B_s] = 2.4 \times 10^{15}$ cm^{-3}	320–360	0.75	1×10^8
[9]	DLTS	p-Si, $[B_s] = 7 \times 10^{15}$ cm^{-3}	309–334	0.8 ± 0.1	1×10^{10}
[10]	TSCAP	p-Si, $[B_s] = 2 \times 10^{14}$ cm^{-3}	290–310	0.70 ± 0.05	3×10^8
[11]	DLTS	n-Si, $[P_s] = 4 \times 10^{14}$ cm^{-3}	263–322	0.71	4×10^8
[12, 13]	Hall effect	n-Si, $[P_s] = 7 \times 10^{13}$ cm^{-3}	280–350	0.77 ± 0.05	2.3×10^7 (Fz-Si)
					9.1×10^9 (Cz-Si)
[16]	IR	p-Si, $[B_s] = 3 \times 10^{13}$ cm^{-3}		0.87	1.4×10^{11}
[17]	DLTS	n-Si, $[P_s] = 9 \times 10^{11}$ cm^{-3}	290–345	0.75	6.2×10^8
[18]	IR	n-Si, $[P_s] = 3 \times 10^{14}$ cm^{-3}	250–300	0.75 ± 0.02	

approximations of the exchange-correlation energy. Before the calculations of the equilibrium C_i defect structure, the lattice constant has been optimized by minimizing the total energy of the supercells. For the Si_{216} supercell, the optimized lattice constant was close to $a = 5.431$ Å.

Further, the carbon atom was placed at an interstitial position in the supercell and the equilibrium configuration was obtained by minimizing the total energy. All the atoms were allowed to relax. It has been found that for all the charge states ($z = 0, +1, -1$) the C_i equilibrium lattice position corresponds to the split $\langle 100 \rangle$ interstitial configuration (with C_{2v} symmetry) and this structure is presented in Fig. 5. The calculated structure of the C_i interstitial is similar to that calculated by other groups [28–31].

For the obtained C_i structure in the neutral charge state ($z = 0$) IR active vibrational modes have been calculated. The calculations were performed in a cluster approximation. The vectors of the normal vibrations are shown in Fig. 5. The calculated frequency values were found to be $v_1 = 853$ cm^{-1} and $v_2 = 925$ cm^{-1} with an intensity ratio $I_1:I_2 = 2:1$. The results obtained are in a reasonable agreement with the experimental data on the frequencies, 922 and 932 cm^{-1}, and the intensity ratio, $I_1:I_2 = 2:1$, of the LVMs due to the C_i defect [3].

Now, we consider the results of our calculation of diffusion coefficient parameters of the interstitial carbon atom. It should be noted that theoretical analysis of the C_i diffusion in previous studies was limited by calculations of a value of diffusion barrier only [29, 30]. Calculated values of the activation barrier for the C_i diffusion are scattered in a rather wide range of energies from 0.5 eV to about 1 eV [29, 30]. The pre-exponential factor for the diffusion coefficient of the interstitial carbon atom was not calculated at all. Here, we present the diffusion coefficient calculation according to the method described in details in Ref. [32]. The diffusion coefficient of the interstitial carbon atom was analyzed on the basis of the general expression obtained by the method of casual wanderings:

$$D = \frac{d^2 N_{et}}{2 d_s} \Gamma, \tag{1}$$

$$\Gamma = \frac{1}{2\pi} \frac{\prod_{i=0}^{N} \gamma_i^{(o)}}{\prod_{i=1}^{N} \gamma_i^{(b)}} \exp\left(-\frac{\Delta E}{k_B T}\right) \tag{2}$$

where d is the diffusion jump distance, N_{et} is the number of the equivalent trajectories from the starting point, d_s is the dimension of space (in our case $d_s = 3$), Γ is the average frequency of jumps to the distance d, ΔE is the adiabatic potential energy difference between the saddle point and the stable configuration, N is a number of atoms in the system, $\lambda_i^{2(o,b)}$ are the eigenvalues of the matrix (with respect to mass-weighted internal coordinates) $K_{ij} = \partial^2 U_{eff}/\partial f_i \partial f_j$. $U_{eff}(f_1 \ldots, fm)$ denotes the potential function as a function of the internal degrees of
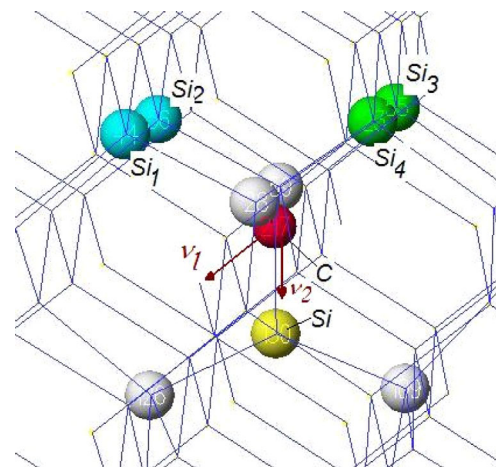

Figure 5 Calculated equilibrium configuration of split $\langle 100 \rangle$ C_i interstitial. v_1, v_2 are the vectors of the normal vibrations.

freedom. The indices (*b*) and (*o*) indicate that the corresponding quantities are evaluated for the saddle point and minimum energy configurations, respectively.

Parameters of the diffusion coefficient are determined by the most probable paths of diffusion and their number (N_{et}). In a general case, for a covalent crystal and diffusing atoms, which strongly interact with a crystal lattice, the most probable diffusion path is the path that connects the two nearest equilibrium configurations of the defect, and movement of the atom along the given path should lead to reconfigurations of the smallest number of covalent bonds. In the case of the interstitial carbon atom, the diffusion paths correspond to transitions in directions of Si(1), Si(2), Si(3), and Si(4) atoms (see Fig. 5), in accordance with the C_{2v} symmetry. Figure 6 shows the variation of the total energy of the supercell ($Si_{64}C$) along one of these paths. The calculation was carried out by minimizing the total energy with the optimization of coordinates of all the atoms. Only the distance between the equivalent configurations was fixed. The calculated values of the diffusion barrier were $\Delta E_{diff} = 0.47$ eV (obtained with the BLYP approximation) and $\Delta E_{diff} = 0.36$ eV (obtained with the LDA approximation).

As it was underlined in Ref. [32], for the determination of the correct value of the diffusion barrier it is necessary to determine the number of silicon atoms (N_{Si}) involved in the process of diffusion. To do this, we have calculated the value of the activation barrier, when only a certain number of silicon atoms N_{Si}, nearest to the diffusion path, has been involved into the minimization of the supercell total energy. Figure 7 shows the activation barrier for C_i diffusion as a function of the number of silicon atoms, N_{si}. An analysis of the results presented in Fig. 7 shows that the value of the diffusion barrier increases with a decrease in the number of silicon atoms
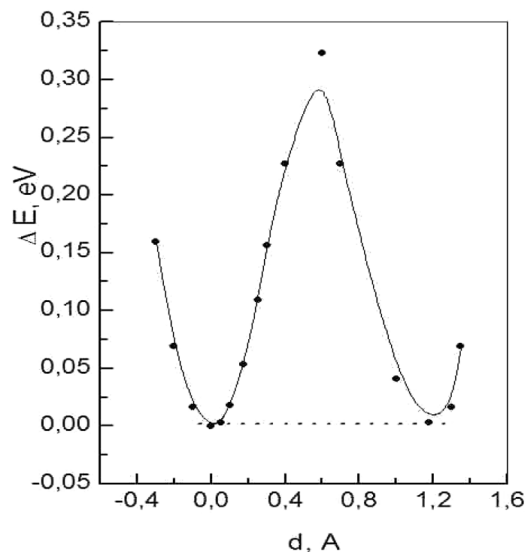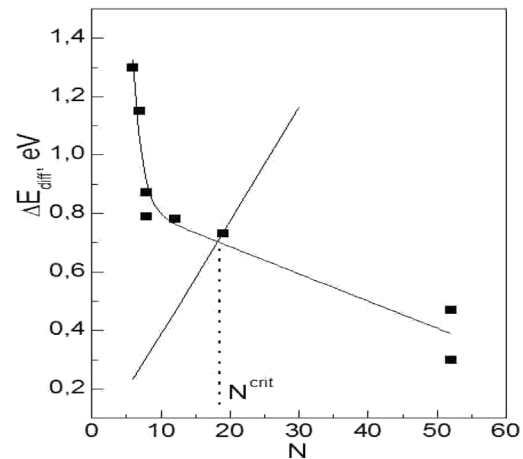

Figure 7 The calculated dependence of the activation barrier on the number of Si atoms (N) involved in the minimization of the total energy of the supercell. The line represent the dependence $E = 3/2 k_B T \times N$, where k_B is the Boltzmann constant, $T_{eff} = 300$ K.

involved in the diffusion process. It should be noted that the calculated dependence $\Delta E_{diff}(N_{Si})$ corresponds to zero temperature. Diffusion processes occur at finite temperatures. The probability of the diffusion transition is determined as the product of the Boltzmann probability (P_B) and the probability (P_N) of forming the optimal configuration of the N nearest silicon atoms. Since P_B decreases and P_N increases with a decrease in N, the product $P_N \times P_B$ has a maximum at N_{Si}^{crit}. So, in order to determine the correct value of the diffusion barrier, one needs to determine the N_{Si}^{crit} value first. The probability of the formation of an optimal configuration can be calculated directly [32]. The N_{Si}^{crit} can be also evaluated in the following way. Suppose we know the value of characteristic temperature (T_{eff}) of a diffusion process (for example, from an experiment). The lower limit of the diffusion barrier at a given temperature is determined then by a point of intersection the curve $\Delta E_{diff}(N_{Si})$ and the line $E = 3/2 \ k_B T_{eff} N_{Si}$. The value of this point on the X-axis (N) corresponds to N_{Si}^{crit} (see Fig. 7).

All configurations of the silicon atoms, located on the right of the point of the intersection N_{Si}^{crit} (Fig. 7) will not be realized due to the thermal motion of the atoms. The correct value of the diffusion barrier $\overline{\Delta E}_{diff}$, can be determined by averaging over all possible configurations of the silicon atoms, located on the left of the point of intersection N_{Si}^{crit}. The calculated values of the activation barrier for diffusion of the interstitial carbon atom in the charge states $z = 0$ and $+1$ are found to be $\overline{\Delta E}_{diff}(z = 0) = 0.74$ eV, $\overline{\Delta E}_{diff}(z = +1) = 0.89$ eV. Since the average is taken over the Boltzmann probability, the average value of the activation barrier is close to the value of the barrier at the intersection N_{Si}^{crit}. It should be noted that $\overline{\Delta E}_{diff}(z = +1) > \overline{\Delta E}_{diff}(z = 0)$. Such a ratio is a consequence of the fact that for the charge state $z = +1$ the saddle point of the diffusion path is shifted further away from the starting equilibrium configuration of the C_i atom.

Figure 6 The calculated dependence of the supercell ($Si_{64}C$) total energy (LDA) on the displacement of carbon atom along the diffusion path.

The calculation of the pre-exponential factor is performed with the use of Eq. (2). The summation has been over 10 silicon atoms closest to the diffusion path. The frequencies ν_i were calculated by numerical differentiation of the total energy of the supercell by shifting ith atom from the equilibrium position. The calculated value of the pre-exponential factor for the diffusion of the interstitial carbon atom in the neutral charge state ($z = 0$) was $D_0 = 0.06$ cm^2 s^{-1}. The calculated values of a pre-exponential factor and the diffusion barriers are in good agreement with the experimental obtained results.

4 Conclusions Experimental and theoretical evidence of a noticeable dependence of the migration ability of the interstitial carbon atom on its charge state are presented in our work. It is found that in a positive charge state the C_i diffusion in crystalline silicon is characterized by the activation energy $\Delta E_a \geq 0.88$ eV, while in a neutral charge state the ΔE_a value is lowered to 0.73–0.74 eV.

References

[1] G. Davies and R. C. Newman, in: Handbook on Semiconductors, edited by T. S. Moss (Elsevier Science, Amsterdam, 1994), Vol. 3b, chap. 21.

[2] K. Kakimoto, B. Gao, S. Nakano, and Y Harada, Jpn. J. Appl. Phys. **56**, 020101 (2017).

[3] A. R. Bean and R. C. Newman, Solid State Commun. **8**, 175 (1970).

[4] L. F. Makarenko, M. Moll, F. P. Korshunov, and S. B. Lastovskii, J. Appl. Phys. **101**, 113537 (2007).

[5] L. I. Khirunenko, M. G. Sosnin, Yu. V. Pomozov, L. I. Murin, V. P. Markevich, A. R. Peaker, L. M. Almeida, J. Coutinho, and V. J. B. Torres, Phys. Rev. B **78**, 150203 (2008).

[6] M. Uematsu, J. Appl. Phys. **111**, 073517 (2012).

[7] G. D. Watkins and K. L. Brower, Phys. Rev. Lett. **36**, 1329 (1976).

[8] L. W. Song and G. D. Watkins, Phys. Rev. **B42**, 5759 (1990).

[9] Y. H. Lee, L. J. Cheng, J. D. Gerson, P. M. Mooney, and J. W. Corbett, Solid State Commun. **21**, 109 (1977).

[10] J. C. Brabant, M. Pugnet, J. Barbolla, and M. Brousseau, J. Appl. Phys. **47**, 4809 (1976).

[11] L. C. Kimerling, P. Blood, and W. M. Gibson, Inst. Phys. Conf. Ser. **46**, 273 (1978).

[12] A. G. Litvinko, L. F. Makarenko, L. I. Murin, and V. D. Tkachev, Fiz. Tekh. Poluprovodn. **14**, 776 (1980) [Sov. Phys. Semicond. **14**, 455 (1980)].

[13] V. P. Markevich and L. I. Murin, Fiz. Tekh. Poluprovodn. **22**, 911 (1988) [Sov. Phys. Semicond. **22**, 574 (1988)].

[14] L. F. Makarenko, F. P. Korshunov, S. B. Lastovskii, L. I. Murin, and M. Moll, Solid State Phenomena **156–158**, 155 (2010).

[15] K. Thonke, A. Teschner, and R. Sauer, Solid State Commun, **61**, 241 (1987).

[16] A. K. Tipping and R. C. Newman, Semicond. Sci. Technol. **2**, 315 (1987).

[17] B. Schmidt, V. Eremin, A. Ivanov, N. Strokan, E. Verbitskaya, and Z. Li, J. Appl. Phys. **76**, 4072 (1994).

[18] M. I. Gritsenko, O. O. Kobzar, Yu. V. Pomozov, M. G. Sosnin, and L. I. Khirunenko, Ukr. J. Phys. **55**, 222 (2010).

[19] L. Dobaczewski, A. R. Peaker, and K. Bonde Nielsen, J. Appl. Phys. **96**, 4689 (2004).

[20] E. V. Monakhov, B. S. Avset, A. Hallen, and B. G. Svensson, Phys. Rev. B **72**, 195207 (2005).

[21] P. Giannozzi, S. Baroni, N. Bonini, M. Calandra, R. Car, C. Cavazzoni, D. Ceresoli, G. L. Chiarotti, M. Cococcioni, I. Dabo, A. Dal Corso, S. de Gironcoli, S. Fabris, G. Fratesi, R. Gebauer, U. Gertsmann, C. Gougoussis, A. Kokalj, M. Lazzeri, L. Martin-Samos, N. Marzari, F. Mauri, R. Mazzarello, S. Paolini, A. Pasquarello, L. Paulatto, C. Sbraccia, S. Scandolo, G. Sclauzero, A. P. Seitsonen, A. Smogunov, P. Umari, and R. M. Wentzcovitch, J. Phys.: Condens. Matter. **21**, 395502 (2009).

[22] H. Djerassi, J. Merlo-Flores, and J. Messier, J. Appl. Phys. **37**, 4510 (1966).

[23] M. A. Green, J. Appl. Phys. **67**, 2944 (1990).

[24] L. C. Kimerling, H. M. DeAngelis, and J. W. Diebold, Solid State Commun. **16**, 171 (1975).

[25] A. O. Evwaraye, J. Appl. Phys. **48**, 734 (1977).

[26] A. O. Evwaraye, J. Appl. Phys. **48**, 1840 (1977).

[27] C. E. Barnes and G. A. Samara, Appl. Phys. Lett. **48**, 934 (1986).

[28] D. J. Backlund and S. K. Estreicher, Phys. Rev. B **77**, 205205 (2008).

[29] R. B. Capaz, A. Dal Pino, Jr., and J. D. Joannopoulos, Phys. Rev. B **50**, 7439 (1994).

[30] F. Zirkelbach, B. Stritzker, K. Nordlund, J. K. N. Lindner, W. G. Schmidt, and E. Rauls, Phys. Rev. B **82**, 094110 (2010).

[31] H. Wang, A. Chroneos, C. A. Londos, E. N. Sgourou, and U. Schwingenschlög, Sci. Reports **4**, 4909 (2014).

[32] V. Gusakov, Solid State Phenomena. **216**, 171 (2014).